JOURNAL OF MATERIALS SCIENCE **40** (2005) 919–926

Grain boundary engineering for superplasticity in steels

T. FURUHARA, T. MAKI
Department of Material Science and Engineering, Kyoto University, Yoshida-honmachi, Sakyo-ku, Kyoto 606-8501, Japan

The microstructure with suitable boundary characters for superplasticity is summarized for the steels which consist of two phases, i.e., ferrite (bcc α) + austenite (fcc γ) or ferrite (α) + cementite (orthorhombic θ-Fe_3C).

In ($\alpha + \gamma$) duplex alloys, a conventional thermomechanical processing (solution treatment + heavy cold rolling + aging) produces the ($\alpha + \gamma$) duplex structure through the competition of recovery/recrystallization of matrix and precipitation. In Fe-Cr-Ni ($\alpha + \gamma$) duplex stainless steels with high γ fractions (40–50%), α matrix undergoes recovery to form α subgrain boundaries and γ phase precipitates on α subgrain boundaries with near Kurdjumov-Sachs relationship during aging. By warm deformation, the transition of α boundary structure from low-angle to high-angle type occurs by dynamic continuous recrystallization of α matrix and, simultaneously, coherency across α/γ boundary is lost. Contrarily, α phase first precipitates in deformed γ matrix in Ni-Cr-Fe based alloy during aging. Subsequently discontinuous recrystallization of γ matrix takes place and the ($\alpha + \gamma$) microduplex structure with high-angle γ boundaries is formed. The formation of those high-angle boundaries in ($\alpha + \gamma$) microduplex structure induces the high strain rate superplasticity.

In an ultra-high carbon steel, when pearlite was austenitized in the ($\gamma + \theta$) region, quenched and tempered at the temperature below A_1, an ($\alpha + \theta$) microduplex structure in which most of α boundaries are of high-angle type is formed through the recovery of the fine (α' lath martensite + θ) mixture during tempering. Such ($\alpha + \theta$) microduplex structure with high angle α boundaries exhibits higher superplasticity than that formed by heavy warm rolling or cold rolling and annealing of pearlite which contains higher fraction of low angle boundaries.

1. Introduction

Grain size refining is important for improving mechanical properties of materials through the grain boundary strengthening, increase in toughness, superplasticity, etc. In fine-grain materials, grain boundary sliding is the most important mechanism of superplasticity. Finer grain size is preferred since the amount of grain boundaries where boundary sliding takes place is large and the distance for accommodation by diffusion and/or slip is shorter. Duplex structure has large advantage for superplasticity since the second phase can inhibit the grain growth of matrix. It should be emphasized, however, that the character of grain boundaries (and of interphase boundaries in multiphase materials) is another key factor for superplasticity in terms of boundary sliding. In this aspect, more disordered boundary structure (those of high-angle grain boundaries or incoherent boundaries) should exhibit good ability of boundary sliding because the density of broken bonds across the boundary is high.

In ferrous alloys, two representative duplex structures exhibit superior fine-grain superplasticity, i.e., ferrite (bcc α) + austenite (fcc γ) structure in duplex stainless steels [1, 2] and in Ni-Cr-Fe alloys [3] and ferrite (α) + cementite (orthorhombic θ-M_3C) structure in ultra-high carbon steels (UHCS) [4]. Recently, the present authors carried out the systematic study to produce fine-grained duplex structure ('microduplex structure') suitable for superplasticity in those materials [5–9]. In those studies, the formation mechanism of high-angle grain boundary through thermomechanical processing combining deformation and phase transformation (precipitation) was especially focused.

The present paper aims to emphasize that the control of grain boundary character is important in the materials with microduplex structures in connection with fine-grain superplasticity.

2. Formation process of microduplex structure with high-angle boundary by thermomehanical processing

2.1. Duplex stainless steel

($\alpha + \gamma$) duplex stainless steels, such as Fe-25%Cr-7%Ni-3%Mo, contain high amount of Cr and Ni. In this steel, the ferrite (α) matrix phase contains a high

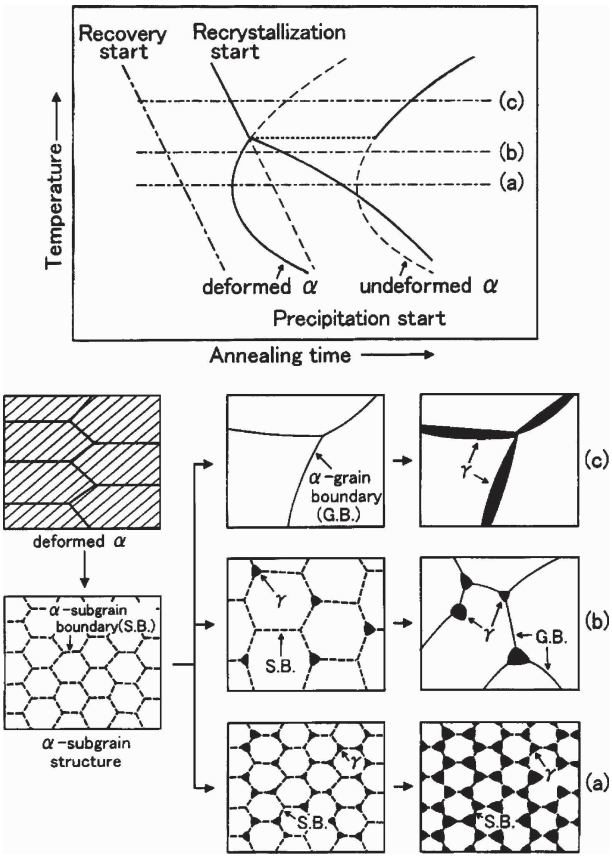

Figure 1 Schematic illustrations of RPTT diagram and the formation process of various ($\alpha + \gamma$) duplex structures during aging of heavily cold-rolled supersaturated α in the Fe-Cr-Ni duplex stainless steel.

volume fraction (40–45%) of austenite (γ). In order to obtain microduplex structures, specimens are solution-treated at higher temperatures in α single-phase region and quenched to obtain a supersaturated α phase at room temperature [10, 11]. The solution-treated specimens are heavily cold rolled (70–90%) and aged at temperatures around 1273 K in ($\alpha + \gamma$) two-phase region.

Fig. 1 schematically shows the formation process of three types of ($\alpha + \gamma$) duplex structure in connection with Recrystallization-Precipitation-Temperature-Time (RPTT) diagram [10]. In the development of this structure, extensive recovery of α matrix occurs resulting in the formation of α subgrain structure prior to γ precipitation. At low aging temperatures (Fig. 1a), γ phase precipitates at α subgrain boundaries. By further holding at lower temperatures, the volume fraction of γ increases to about 0.4 and the microduplex structure consisting of fine α subgrain matrix and fine γ precipitates is obtained. At high aging temperatures (Fig. 1b), the volume fraction of γ is small and hence recrystallization of α subgrain matrix occurs by prolonged aging because a pinning effect by γ precipitate is reduced. This results in the coarse two-phase structure consisting of large recrystallized α grains and fairly large γ particles as shown in Fig. 1b. Furthermore, when aging is performed at much higher temperatures, the recrystallization of α matrix occurs prior to γ precipitation, resulting in coarse α grains and film-like γ precipitates formed along α grain boundaries (Fig. 1c).

Superplasticity is observed for the microduplex structure such as Fig. 1a with high volume fraction of γ precipitate. Fig. 2a to c show the change in ($\alpha + \gamma$) microduplex structure of Fe-26%Cr-8%Ni during tensile deformation at 1273 K at the strain rate of 1.7×10^{-2} s^{-1}. Before deformation (Fig. 2a), the sizes of α subgrains and γ particles are about 1 μm, and dislocations are scarcely observed within α subgrains. After 20% tensile deformation (just after the peak stress was obtained in the stress-strain curve), a fair amount of dislocations are introduced within α subgrains (Fig. 2b). In the specimen deformed in tension by 100%, on the other hand, dislocations are again rarely seen (Fig. 2c) and the misorientation between adjacent α grains is large. Fig. 2d shows transmission electron microstructures of Fe-26Cr-5Ni in which the volume fraction of γ phase is 20% immediately quenched after 100% deformation at 1273K. Initially, the 5Ni and 8Ni alloys were similar in both of α subgrain size and γ particle size. Dislocation density is fairly high in α matrix of Fe-26Cr-5Ni although microstructure is almost dislocation-free in Fe-26Cr-8Ni of Fig. 2c. This implies that deformation occurs by intragranular slip in Fe-26Cr-5Ni whereas the dominant deformation mechanism is grain boundary sliding in Fe-26Cr-8Ni.

Fig. 3a shows a change in the misorientation across α boundary during the early tensile deformation up to 100%. It appears that the misorientation of α subgrains gradually increases with an increase in the amount of deformation and most of α boundaries become high-angle boundaries. The misorientation from Kurdjumov-Sachs (K-S) orientation relationship between α matrix and γ article (Fig. 3b) is also gradually increased as the tensile deformation proceeds indicating that α/γ interphase boundaries lose their coherency. It clearly indicates that the boundary structure suitable for boundary sliding can be formed during the early stage of deformation in ($\alpha + \gamma$) duplex stainless steels. This microstructure change occurs through dynamic continuous recrystallization of α matrix [5, 6, 12].

It was demonstrated this kind of microduplex structure exhibits superplastic elongation over 2500% at a strain rate of 4×10^{-3} s^{-1} [1] and over 1000% even at a high strain rate such as 1.7×10^{-1} s^{-1} [5]. Fig. 4a shows total elongation at 1273 K and an initial strain rate of 1.7×10^{-2} s^{-1} for different volume fraction of γ in various Fe-26Cr-Ni alloys. Large elongation over 800% is obtained in the cases of Fe-26Cr-8Ni and 9Ni alloys with γ volume fractions of nearly 50%. As γ volume fraction decreases, elongation decreases and only 240% in Fe-26Cr-5Ni of which γ volume fraction is 20%. When tensile tests are performed at various strain rates, elongation is larger as the amount of γ was larger for each strain rate as is shown in Fig. 4b. It is clear that γ volume fraction should be large as about 40–50% for the appearance of superior superplasticity in ($\alpha + \gamma$) microduplex structures of Fe-26Cr-Ni alloys.

The possible reasons for poor superplasticity for the alloy with small γ volume fraction may be as follows. First, α subgrain growth is faster due to smaller pinning force when γ interparticle spacing is larger. Therefore,

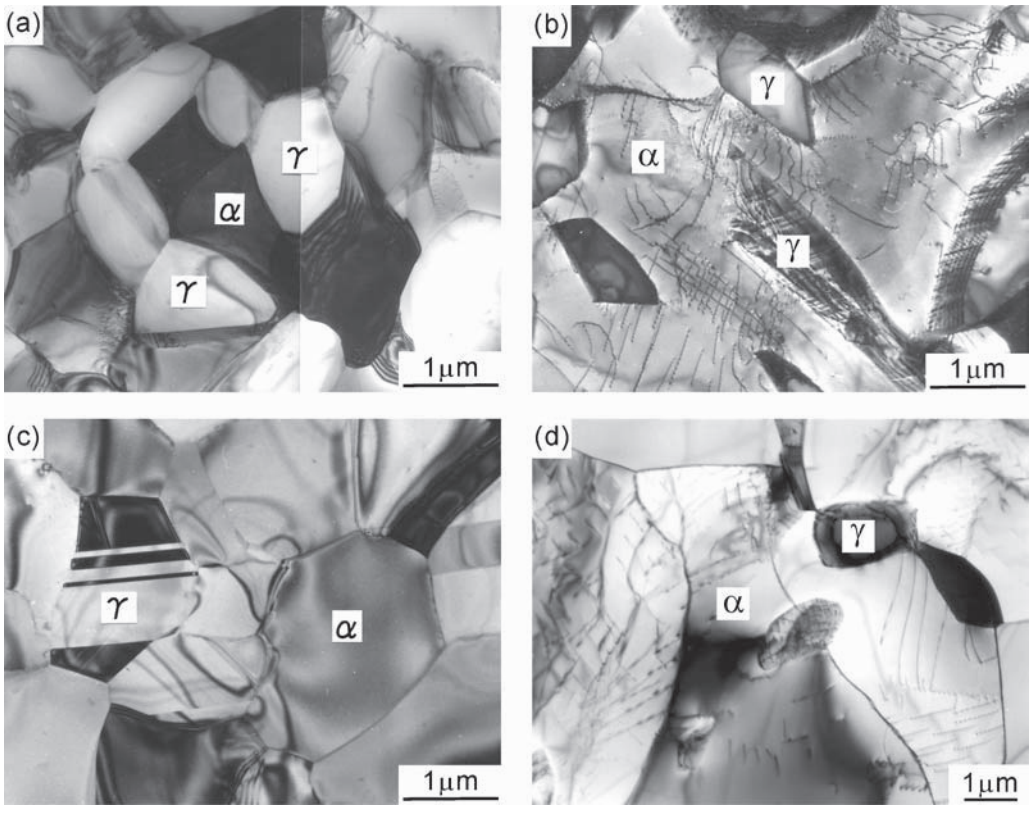

Figure 2 Transmission electron microstructure of the Fe-26Cr-Ni alloys after cold rolled by 85% and annealed at 1273 K for 60 s, (a) as-annealed condition and (b), (c) after 20 and 100% deformation at 1273 K (the initial strain rate of 1.7×10^{-2} s^{-1}), respectively, for Fe-26Cr-8Ni and (d) after 100% deformation at the initial strain rate of 1.7×10^{-2} s^{-1} for Fe-26Cr-5Ni.

α subgrain size in the case of a smaller γ fraction becomes larger during deformation. Secondly, γ particles, which are harder than α matrix in the temperature range between 1073 to 1273 K [13], induce heterogeneous deformation with the operation of multiple slip systems around themselves in α, resulting in the increase of α boundary misorientation by absorbing those dislocations, i.e., dynamic continuous recrystallization of α [12]. When the amount of γ is small, less heterogeneous deformation would be introduced to the microstructure. Thus, the transition of α subgrain boundaries to high angle boundaries is slower in the alloys with larger γ interparticle spacing. Those reasons lead to the decrease in the contribution of grain boundary sliding in deformation and hence the necking of the specimen occurs in the early stage of deformation before α subgrains turn to the grains with high angle boundaries, resulting in poor superplastic behavior especially of Fe-26Cr-5Ni. It was confirmed by Kikuchi pattern analysis that α matrix exhibits a subgrain structure in the specimen of Fe-26Cr-5Ni even after 100% deformation [7] whereas initial α subgrain boundaries turn mostly to high angle grain boundaries after 100% elongation in Fe-26Cr-8Ni as shown in Fig. 3. These results confirm that the transition of α subgrain boundaries to high angle ones through dynamic continuous recrystallization is more difficult in the $(\alpha + \gamma)$ microduplex structure with a smaller γ volume fraction. In addition, it was pointed out that α/γ interphase boundary sliding is faster by the factor of 10^2 to 10^3 than α/α and γ/γ grain boundaries [13]. Larger fraction of α/γ interphase boundary in the total amount of boundary contained may be responsible for better superplastic performance in the alloys with a larger γ volume fraction.

2.2. Ni-Cr-Fe alloys

Hayden *et al.* [3] reported superior superplasticity over 1000% in elongation for $(\alpha + \gamma)$ microduplex structures with γ grain size of about 3 μm in Ni-Cr-Fe alloys in which about 10 vol% of α phase precipitates from γ matrix at 1255 K. The present authors studied the formation process of $(\alpha + \gamma)$ microduplex structure in a Ni-40%Cr-6%Fe-2%Ti-1%Al alloy with γ matrix through thermomechanical processing (solution treatment + heavy cold rolling + aging) [7].

Transmission electron microstructures of Fig. 5 show the microstructure change in the heavily cold rolled specimens during subsequent aging. Deformed γ matrix contains high densities of dislocations and deformation twins. By heating to aging temperature, deformed γ starts to recrystallize and form fine-grained structure. Fig. 5a shows that α phase particles, of which size is about few tens of nanometers in size, precipitate at deformation twin boundaries and presumably dislocations in deformed γ matrix during heating to 1073 K. On the other hand, the recrystallized area exhibits a fine $(\alpha + \gamma)$ microduplex structure, which consists of γ grains and α precipitates with diameters of about 0.1 μm (Fig. 5b). By further heating and holding at 1273 K, the fraction of recrystallized γ area increases and recrystallized γ grains grow fast to the sizes of nearly 1 μm in diameter. Fig. 5c shows transmission

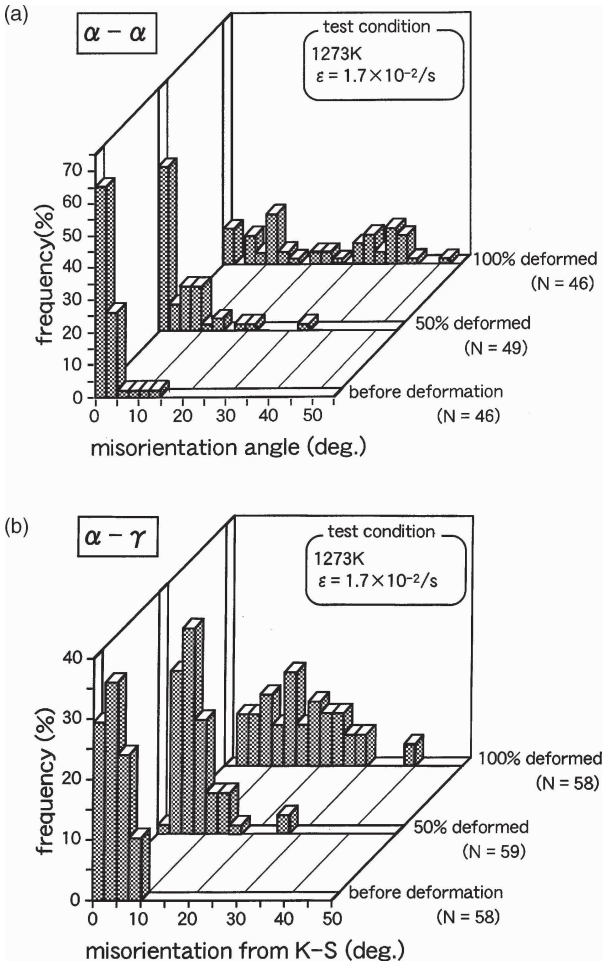

Figure 3 Histograms showing the change of misorientation between (a) α grain boundary and (b) α/γ interphase boundary from K-S relationship during tensile deformation at 1273 K (the initial strain rate of 1.7×10^{-2} s^{-1}) in Fe-26Cr-8Ni.

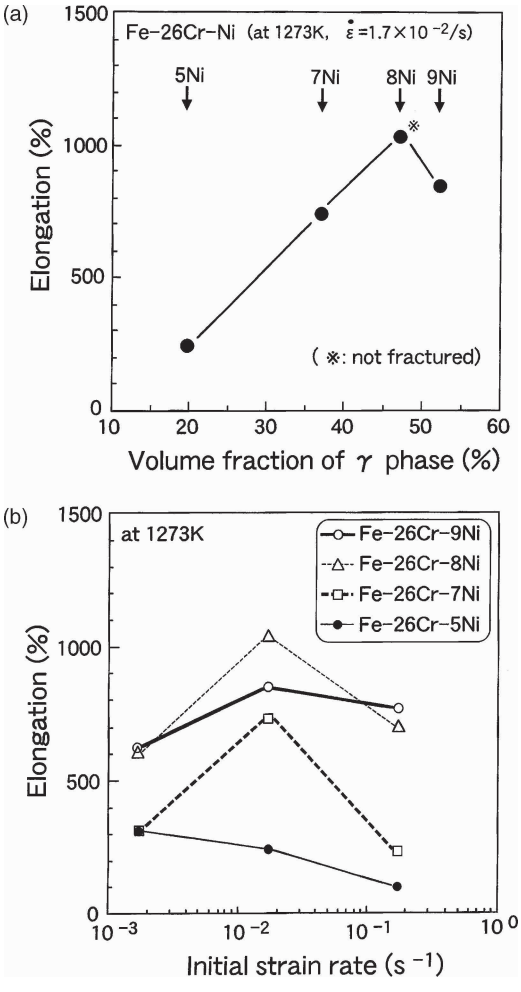

Figure 4 Tensile properties of the Fe-26Cr-Ni specimens at 1273 K; (a) total elongation vs. γ volume fraction at the initial strain rate of 1.7×10^{-2} s^{-1}; (b) total elongation vs. initial strain rate.

electron micrograph of the $(\alpha + \gamma)$ microduplex structure in the specimen held at 1273 K for 1.8 ks. Average grain size of γ is 1.5 μm. α precipitates with the average particle size of 0.6 μm are mostly located at γ matrix boundaries whereas some intragranular α phase which precipitated or were embedded by recrystallized γ grains, are seen occasionally. This implies that grain growth of recrystallized γ is suppressed by the pinning of α precipitate. Fig. 5d shows the grain boundary characters in γ phase determined by Kikuchi pattern analysis. Most of γ grain boundaries are high-angle ones with misorientation larger than 15 degrees. Thus, discontinuous recrystallization of γ and suppression of γ grain growth by α is responsible for the formation of $(\alpha + \gamma)$ microduplex structure with high-angle grain boundaries. Rational orientation relationships which α phase originally satisfied with respect to the deformed γ matrix would be lost by recrystallization of γ matrix. The coherency across α/γ interphase boundary decreases significantly through this microstructure change.

Fig. 6 shows the tensile properties at 1273 K for the specimens held at 1273 K for 1.8 ks after 85% cold rolling. Large elongation is obtained even at a high strain rate of 1.7×10^{-1} s^{-1}. Fig. 6b shows that flow stress increases as strain rate increases. Strain rate sensitivity exponent (m) is larger than 0.4 in the whole range of strain rates at which tensile test was conducted. The high strain rate superplasticity in this alloy was observed for the first time in the present study. The high-angle γ boundaries and α/γ boundaries of poor coherency formed by discontinuous recrystallization of γ largely contributes to the superplasticity in these materials.

2.3. Ultra-high carbon steels (UHCS)

Superplasticity in UHCS is achieved for the $(\alpha + \theta)$ microduplex structure with fine, spheroidized θ (Fe_3C) particles dispersed in fine-grained α matrix. Sherby *et al.* [4, 14–18] developed such $(\alpha + \theta)$ microduplex structure by rather complicated thermomechanical processing. The process they proposed consists of three steps; (1) heavy hot rolling in the $(\gamma + \theta)$ two phase region after austenitizing; (2) heavy warm rolling at the temperature just below A_1 temperature; (3) quenching and tempering below A_1 after austenitizing in the $(\gamma + \theta)$ region. The $(\alpha + \theta)$ microduplex structure which exhibits superplasticity was also produced by heavy cold rolling and annealing of pearlite [19].

The present authors studied the microstructure change of the UHCS (Fe-1.0%C-1.4%Cr) in various kinds of thermomechanical processing; (a) the heavy

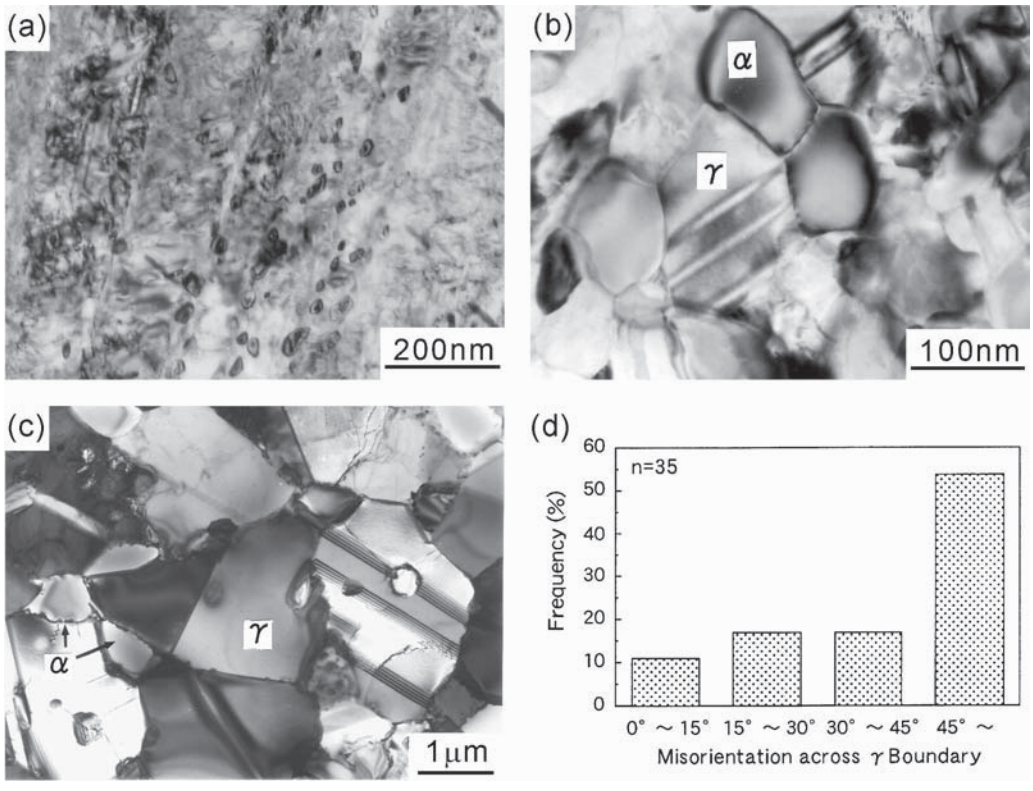

Figure 5 Transmission electron microstructures of Ni-40Cr-6Fe-2Ti-1Al; (a) microstructure in the deformed γ area and (b) $(\alpha + \gamma)$ microduplex structure in the recrystallized γ area in the specimen cold rolled by 85%, heated to 1073 K by 1 K/s and immediately quenched, respectively. (c) $(\alpha + \gamma)$ microduplex structure and (d) the corresponding distribution of γ grain boundary character in the specimen held at 1273 K for 1.8 ks.

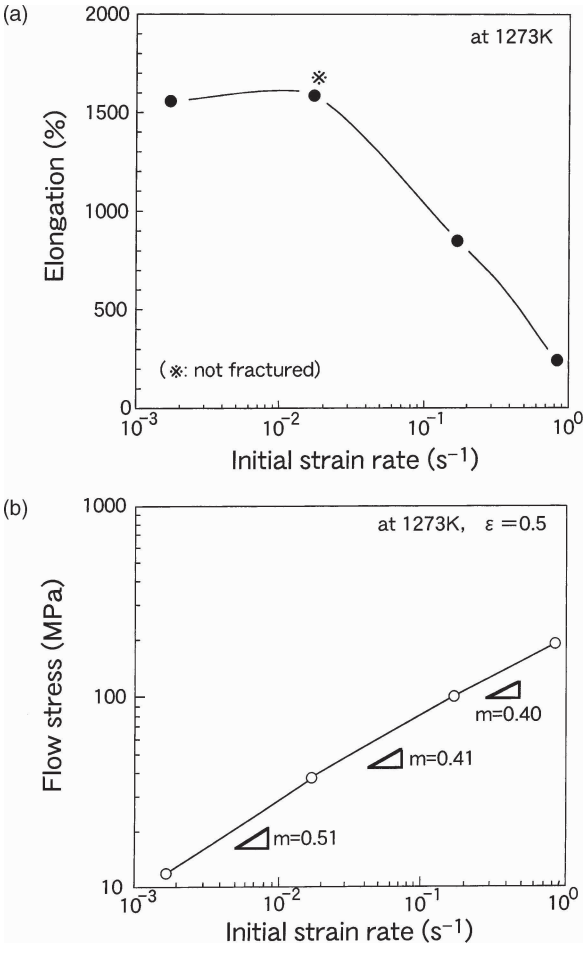

Figure 6 Tensile properties of the Ni-40Cr-6Fe-2Ti-1Al specimens at 1273 K with various initial strain rates; (a) superplastic elongation; (b) flow stresses at the strain of 0.5.

warm rolling of pearlite below A_1 temperature (WR), (b) the annealing below A_1 after heavy cold rolling of pearlite (CR+A) and (c) the austenitizing in the $(\gamma + \theta)$ region between A_{cm} and A_1 followed by quenching and tempering below A_1 (QT); shown in Fig. 7.

Fig. 8a shows the transmission electron micrograph of the specimen warm-rolled by 90% at 923 K (WR). An ultra-fine $(\alpha + \theta)$ duplex structure is developed by warm rolling of the pearlite structure. The average α grain size is 0.43 μm and the average θ particle size is 0.18 μm, both in diameter. Fig. 8b shows the histogram of misorientation angle across the α grain boundaries in the warm-rolled specimen. Majority of α grain boundaries are of low-angle one with misorientations less than 15 degrees.

Fig. 9a shows the transmission electron micrograph of the $(\alpha + \theta)$ duplex structure in the specimen annealed at 973 K for 0.6 ks after 90% cold rolling of the pearlite structure (CR+A). The annealed structure consists of the coarse-grain region with α grain size of about 0.4 μm and the fine-grain region with α grain size of about 0.2 μm. The illustrations of Fig. 9b and c show the grain boundary characters for each of those regions, respectively. The coarse-grain region in (b) contains many high-angle boundaries with misorientations larger than 15 degrees. On the other hand, most of α grains are subgrains surrounded by low-angle boundaries in the fine-grain region in (c). TEM examination in the early stage of annealing revealed that the area with large misorientations in the deformed α turn to be the coarse-grain region with high-angle α boundaries after recovery during annealing [20].

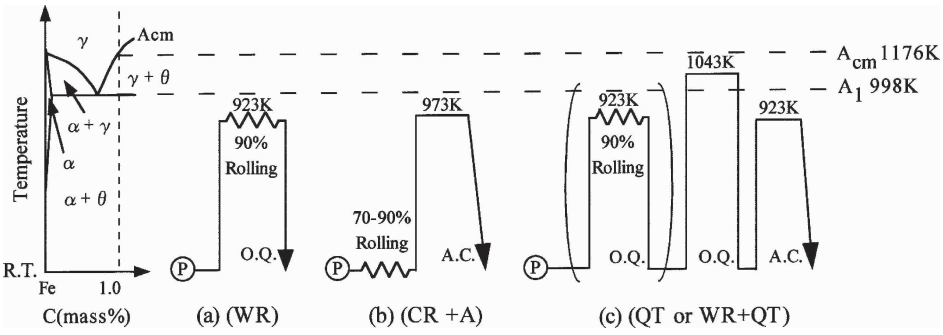

Figure 7 Thermomehanical processing performed for an Fe-1.0C-1.4Cr alloy. (a) 90% warm rolling of pearlite structure at 923 K (WR); (b) annealing at 973 K after 70–90% cold rolling of pearlite structure (CR+A); (c) austenitizing at 1043 K of pearlite structure + quenching + tempering at 923 K without or after 90% warm rolling at 923 K (QT or (WR + QT), respectively).

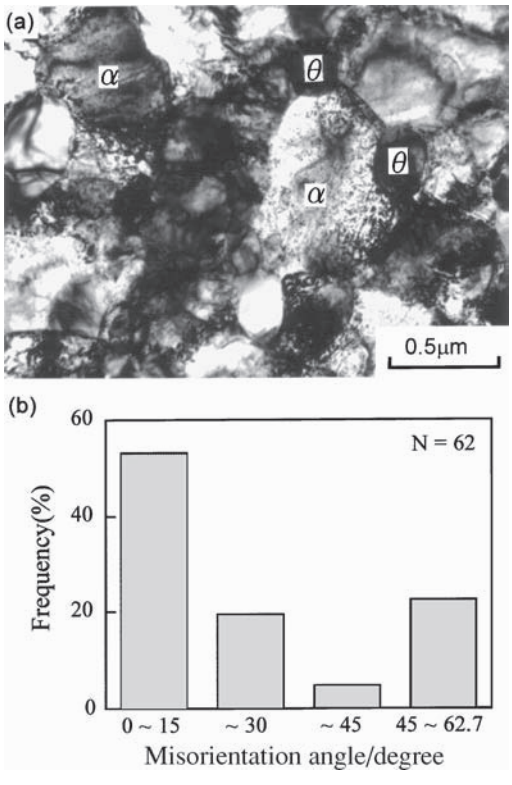

Figure 8 (a) Transmission electron micrograph of the $(\alpha + \theta)$ microduplex structure and (b) distribution of misorientation angle across α grain boundaries in the WR specimen of Fe-1.0C-1.4Cr.

The transmission electron micrographs of Fig. 10 show the microstructure change in the QT treatment. In austenitizing treatment at 1043 K in the $(\gamma + \theta)$ region, the mixture of γ grains and undissolved θ particles is obtained. The average γ grain size is relatively small (about 11 μm) due to the pinning effect by θ particles. γ matrix transforms to α' lath martensite during quenching from 1043 K. Lath martensite structure consists of "block" (a group of laths with almost the same orientation) and "packet" (a group of laths with almost the same habit plane) structures [22]. In Fig. 10a, the growth of lath martensite seems to be disturbed by the undissolved θ particles in γ grains. As a result, blocks are significantly refined in comparison with the case without θ particles. After tempering at 923 K (Fig. 5b), these undissolved θ particles grow and new θ particles also precipitate in martensite (see the arrows), resulting in a bimodal distribution of θ particle size in the final $(\alpha + \theta)$ structure. Simultaneously, the recovery of lath martensite proceeds to form subboundaries in the block. Since block or packet boundaries are mostly high-angle boundaries [23], the migration of block and packet boundaries occurs in some extent even with the pinning by θ particles. Thus, by further tempering, the shape of α grains changes to equi-axed and, finally, an ultra-fine $(\alpha + \theta)$ duplex structure is developed as shown in Fig. 10c. The average grain sizes are 0.40 μm for α and 0.18 μm for θ is developed, respectively, which are similar to those in the WR specimen. However, the histogram of misorientation angles across the α grain boundaries in Fig. 10d indicates that most of α boundaries are high-angle ones with misorientation larger than 15 degrees. In the initial pearlite, there are low energy orientation relationships between ferrite and cementite. Those relationships would be lost during the reverse transformation to austenite and the martensitic transformation subsequently occurred. Thus, it is considered that α/θ interphase boundaries are with poor coherency in this duplex structure.

Heavy warm rolling before QT treatment is effective to obtain fine and uniform γ structure because

TABLE I Formation mechanism of high-angle matrix boundaries and the role of second phase in the fine-grained superplasticity of the steels which consist of two phases.

System	Matrix phase	Second phase	Formation mechanism of high-angle boundary in matrix	Role of second phase for superplasticity
Fe-Cr-Ni	Ferrite (α)	Austenite (γ)	Dynamic continuous recrystallization	Heterogeneous matrix deformation around precipitate Suppression of matrix grain growth
Ni-Cr-Fe	Austenite (γ)	Ferrite (α)	Static discontinuous recrystallization	Pinning of matrix grain growth
UHCS	Ferrite (α)	Cementite (θ)	Martensitic transformation and recovery of martensite	Grain refining of γ matrix Inhibition of martensite block growth Suppression of α grain growth

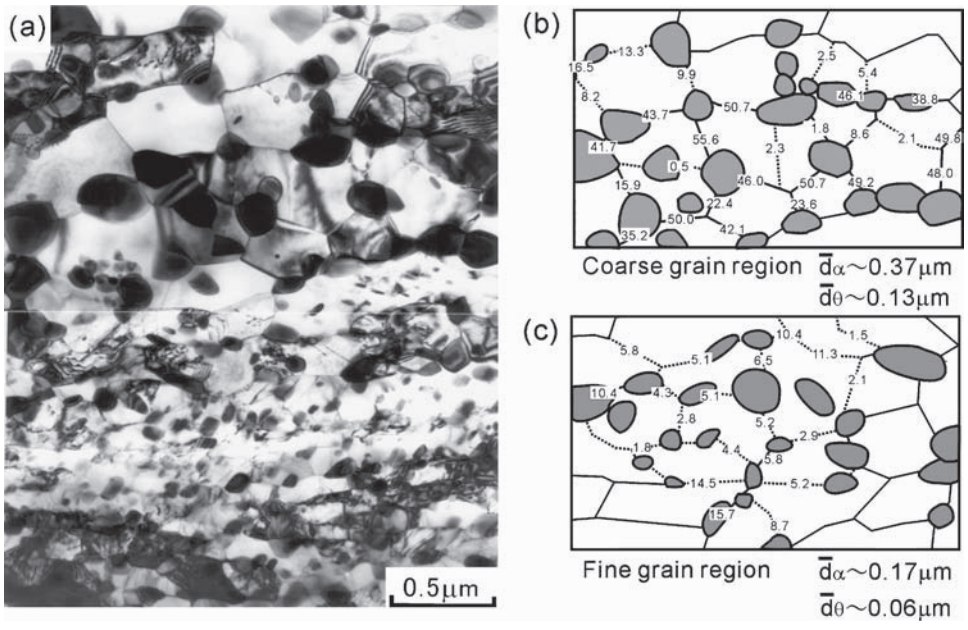

Figure 9 (a) Transmission electron micrograph of the $(\alpha + \theta)$ microduplex structure and (b), (c) misorientation angles across α grain boundaries in the coarse-grain and fine-grain regions in the (CR+A) specimen of Fe-1.0C-1.4Cr, respectively.

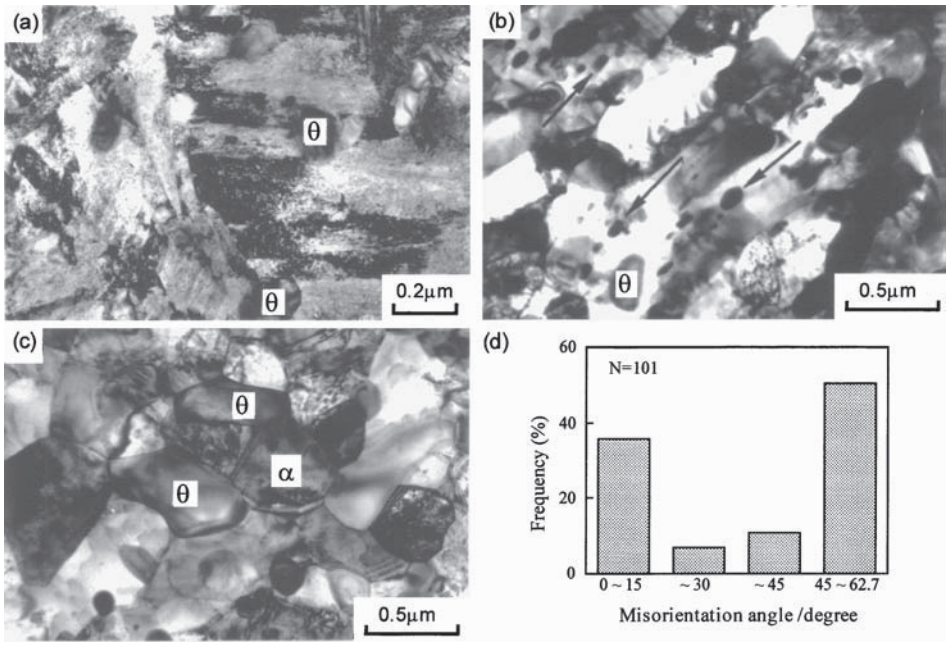

Figure 10 Microstructure change in the QT treatment; (a) as-quenched, (b) after tempering at 923 K for 0.6 ks and (c) for 1.8 ks, respectively, (d) distribution of misorientation angle across α grain boundaries.

the dispersion of cementite particles becomes finer and more uniform by the heavy warm rolling. Uniformly distributed fine θ particles should lead to the higher nucleation rate of γ and the larger pinning effect to suppress γ grain growth.

The result of tensile test at 973 K for those specimens is summarized in Fig. 11. The QT specimen exhibits more than 500% elongation at the strain rate of 1.7×10^{-4} s^{-1} although the addition of warm rolling (WR + QT) results in further improvement of superplastic performance. The (WR+QT) and QT specimens which contain large proportions of high-angle α grain boundaries show much better superplastic properties than the WR specimens with low-angle α boundaries (about 300% elongation at the strain rate of 1.7×10^{-4} s^{-1}). In the (CR+A) specimens, two kinds of microduplex structures, i.e., the coarse-grain region with high-angle α boundaries and the fine-grain region with low-angle α boundaries, are mixed. The resultant superplastic performance is poorer than the (WR + QT) and QT specimens but better than the WR specimen. This result clearly indicates that larger fractions of high-angle α grain boundaries which are capable of grain boundary sliding are of great importance for superplasticity in the ultra-high carbon steels with $(\alpha + \theta)$ microduplex structures.

It is concluded that, in UHCS, the reverse transformation of pearlite to austenite and the martensitic transformation by quenching are responsible for the formation of the $(\alpha + \theta)$ microduplex structure with a large fraction of high-angle α grain boundaries.

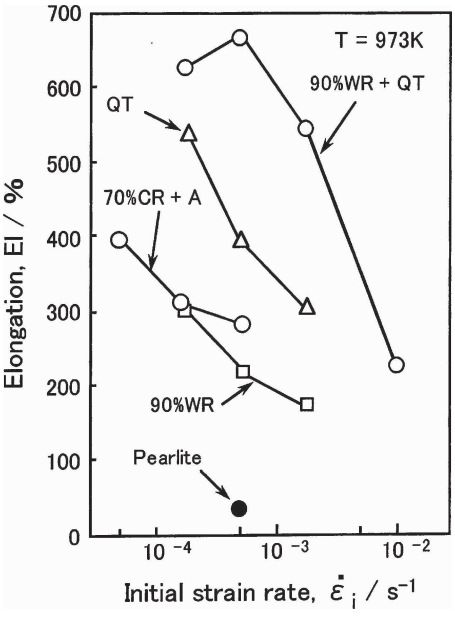

Figure 11 Elongation to failure of the specimens on which various thermomechanical processings were performed (deformed in tension at 973 K and at various initial strain rates).

3. Summary

In the present paper, the methods to produce grain boundary (and interphase boundary) characters suitable for fine-grain superplasticity in three kinds of steels are reviewed. Table I summarizes the formation mechanisms of high-angle boundaries in the matrix and the role of second phase for microstructure development. Recrystallization of matrix is needed for superplasticity of $(\alpha + \gamma)$ microduplex structure whereas phase transformation plays the most important role in UHCS. The volume fraction of second phase is also important to increase the fraction of high-angle boundaries and the refining of grain size.

Recently, dynamic continuous recrystallization calls more attention in the production of ultra-fine-grained structure with high-angle boundaries, which gives high-strength without losing toughness, by heavy deformation processes [24, 25]. Such novel methods to control grain boundary structure should be more widely applied in future materials research.

References

1. Y. MAEHARA, *Trans. ISIJ* **25** (1985) 69.
2. Y. MAEHARA and Y. OHMORI, *Metall. Trans. A* **18A** (1987) 663.
3. H. W. HAYDEN, R. C. GIBSON, H. F. MERRICK and J. H. BROPHY, *Trans. ASM* **60** (1967) 3.
4. J. WADSWORTH and O. D. SHERBY, *J. Mater. Sci.* **13** (1978) 2645.
5. K. TSUZAKI, H. MATSUYAMA, M. NAGAO and T. MAKI, *Mater. Trans. JIM* **31** (1990) 983.
6. T. YAMAZAKI, Y. MIZUNO, T. FURUHARA and T. MAKI, *Mater. Sci. Forum* **304–306** (1999) 127.
7. T. FURUHARA, Y. MIZUNO and T. MAKI, *Mater. Trans. JIM* **40** (1999) 815.
8. E. SATO, S. FURIMOTO, T. FURUHARA, K. TSUZAKI and T. MAKI, *Mater. Sci. Forum* **304–306** (1999) 133.
9. T. FURUHARA, E. SATO, T. MIZOGUCHI, S. FURIMOTO and T. MAKI, *Mater. Trans.* **43** (2002) 2455.
10. K. AMEYAMA, K. MURAKAMI, T. MAKI and I. TAMURA, *J. Jpn. Inst. Met.* **49** (1985) 1045.
11. T. MAKI, T. FURUHARA and K. TSUZAKI, *ISIJ Inter.* **41** (2001) 571.
12. K. TSUZAKI, HUANG XIAOXU and T. MAKI, *Acta Metall. Mater.* **44** (1996) 4491.
13. S. HASHIMOTO, F. MORIWAKI, T. MIMAKI and S. MIURA, in "Superplasticity in Advanced Materials," edited by S. Hori, M. Tokizane and N. Furushiro (The Japan Society for Research on Superplasticity, 1991) p. 23.
14. O. D. SHERBY, B. WALSER, C. M. YOUNG and E. M. CADY, *Scripta Metall.* **9** (1975) 569.
15. B. WALSER and O. D. SHERBY, *Metall. Trans. A* **10A** (1979) 1461.
16. O. D. SHERBY, T. OYAMA, D. W. KUM, B. WALSER and J. WADSWORTH, *J. Metals* **37** (1985) 50.
17. D. R. LESURE, C. M. SYN, A. GOLDBERG, J. WADSWORTH and O. D. SHERBY, *ibid.* **45** (1993) 40.
18. T. OYAMA, O. D. SHERBY, J. WADSWORTH and B. WARSER, *Scripta Metall.* **18** (1984) 799.
19. K. SETO, T. KATO and H. ABE, *Mat. Res. Symp. Proc.* **196** (1990) 99.
20. T. MIZOGUCHI, T. FURUHARA and T. MAKI, in Proc. Int. Symp. on Ultra-Fine Grained Steels (ISIJ, 2001), 198.
21. S. TAGASHIRA, K. SAKAI, T. FURUHARA and T. MAKI, *ISIJ Inter.* **40** (2000) 1149.
22. T. MAKI, K. TSUZAKI and I. TAMURA, *Trans. ISIJ* **20** (1980) 207.
23. T. MAKI, S. MORITO and T. FURUHARA, in Proc. 19th ASM Heat Treat. Soc. Conf. (ASM International, Materials Park, OH, 2000) p. 631.
24. A. OHMORI, S. TORIZUKA, K. NAGAI, K. YAMADA and Y. MUKAIGO, *Tetsu-to-Hagane* **88** (2002) 857.
25. G. KELLY, H. BELADI and P. D. HODGSON, *ISIJ Inter.* **42** (2002) 1585.